Supporting Information

Fischer et al. 10.1073/pnas.1011995108

SI Text

Comparison with DynDom. It is interesting to describe what a widely used tool such as DynDom (1) gives for the transition. DynDom relates two conformations by decomposing the protein into multiple domains and assigns to each domain an independent screw axis (i.e., a combined translation/rotation axis). When provided with the T and R structures of hemoglobin, DynDom finds only a single screw axis (13° rotation, 1.6-Å translation) relating one αβ-dimer to the other (very similar to the 15° axis of Baldwin and Chothia (2), Fig. 1*A*). This axis does not coincide with any element of secondary structure. The reason DynDom does not identify the rotation axes of Q1 and Q2 of hemoglobin is that the same region of the protein (e.g., α_1) is part of two different domains moving successively in different ways (i.e., first α_1 rotates by itself during Q1; then it is part of the $\alpha_1\beta_1$-domain during the Q2 rotation). Moreover, the domains of Q2 ($\alpha_1\beta_1$ and $\alpha_2\beta_2$) are modified by Q1 (motion of subunits α_1 and α_2 relative to $\beta_1\beta_2$).

Note that when the knowledge about the intermediate structures found here along the minimum energy path is used, for example, by providing DynDom with T structure and the $\lambda = 0.5$ intermediate, DynDom does find the domains and rotation axes of Q1 (identifying helix αG as the hinge). Similarly, when provided with the $\lambda = 0.5$ intermediate and the R structure, DynDom finds the elements of Q2 (identifying helix αH as the hinge). This indicates that DynDom can be used as diagnostic tool in the study of large-scale conformational change to identify cases in which the actual motion involves interdependent domains: When the hinge found by DynDom using only the two end states is not related to an element of secondary structure, this is an indication that the motion might be complex. The transition can then be analyzed further, for example, by computing the unbiased minimum energy path by conjugate peak refinement (CPR) (3). If the transition is very complex, it may be useful to characterize it by building a transition network on the high-dimensional landscape of the protein energy (4).

Experimental Suggestions to Capture the Q1 and Q2. This unsuspected pathway could be verified by capturing the intermediate state between Q1 and Q2 using allosteric effectors that potentially uncouple the two quaternary transitions. For example, a covalently liked derivative of inositol hexaphosphate (IHP), which binds between the two β-subunits and inhibits the transition from the T state to the R state (5), could be used in such experiments. The comparison of the structures from the CPR calculations with the IHP-bound hemoglobin X-ray structure (6) shows that the IHP molecule overlaps with the hemoglobin residue only after Q2 (Fig. S2), implying that the Q1 transition could occur without the release of IHP because only the α-subunits undergo a significant displacement in Q1. The Q2 transition, which primarily involves the β-subunits and closes the central cavity where IHP (and 2,3-bisphosphoglycerate) binds, would not be able to take place.

Alternatively, single molecule spectroscopy, combined with FRET measurements of structural changes (7–9), could be used to obtain information that supports the proposed transition mechanism (see Fig. S4 for proposed labeling sites). However, high precision multiple color FRET measurements, beyond those feasible at present, will be required because the rmsd between the standard (Baldwin–Chothia path) and the new path is always less than 1.2 Å (see Fig. S3).

1. Hayward S, Berendsen HJC (1998) Systematic analysis of domain motions in proteins from conformational change: New results on citrate synthase and T4 lysozyme. *Proteins* 30:144–154.
2. Baldwin J, Chothia C (1979) Haemoglobin: Structural changes related to ligand binding and its allosteric mechanism. *J Mol Biol* 129:175–220.
3. Fischer S, Karplus M (1992) Conjugate peak refinement: An algorithm for finding reaction paths and accurate transition-states in systems with many degrees of freedom. *Chem Phys Lett* 194:252–261.
4. Noe F, Krachtus D, Smith JC, Fischer S (2006) Transition networks for the comprehensive characterization of complex conformational change in proteins. *J Chem Theory Comput* 2:840–857.
5. Arnone A, Perutz MF (1974) Structure of inositol hexaphosphate-human deoxyhaemoglobin complex. *Nature* 249:34–36.
6. Waller DA, Liddington RC (1990) Refinement of a partially oxygenated T state human haemoglobin at 1.5 A resolution. *Acta Crystallogr B* 46:409–418.
7. Abbondanzieri EA, et al. (2008) Dynamic binding orientations direct activity of HIV reverse transcriptase. *Nature* 453:184–189.
8. Tarsa PB, et al. (2007) Detecting force-induced molecular transitions with fluorescence resonant energy transfer. *Angew Chem Int Edit* 46:1999–2001.
9. Merchant KA, Best RB, Louis JM, Gopich IV, Eaton WA (2007) Characterizing the unfolded states of proteins using single-molecule FRET spectroscopy and molecular simulation. *Proc Natl Acad Sci USA* 104:1528–1533.

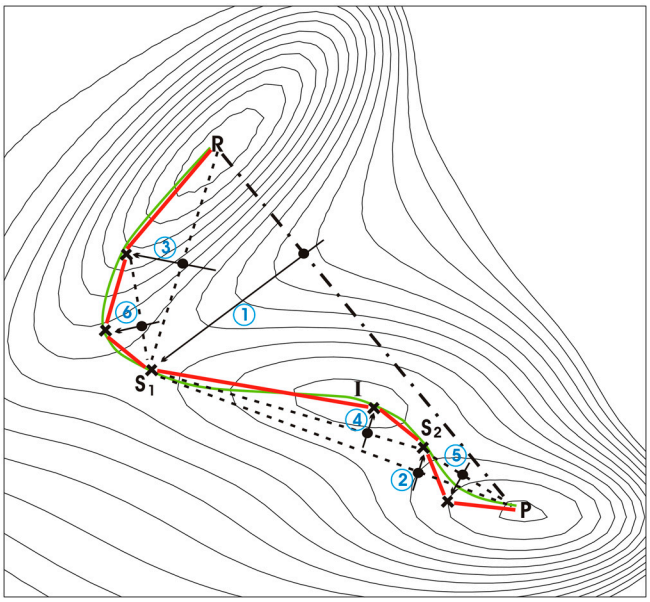

Fig. S1. Progress of a CPR of a minimum energy path (MEP). Contour levels show the energy landscape of a hypothetical molecule (with minima at R, I, and P). The initial guess of the path is taken here as the straight interpolation line (– · –) from the reactant (R) to the product (P) states (results do not depend on whether the transition is considered as R → P or P → R). Each CPR cycle (cycles are numbered) automatically adds (•) and optimizes (↓) intermediate structures (**X**) until the joining path segments (- - -) describe a final path (**X**—**X**, in red) that goes through the exact saddle point (S_1 , S_2) and is near the MEP (in green). The high-dimensional energy surface of a protein has many MEPs. Because path intermediates are removed in some CPR cycles (not shown here), MEPs with high barriers are mostly avoided (see ref. 3 for details).

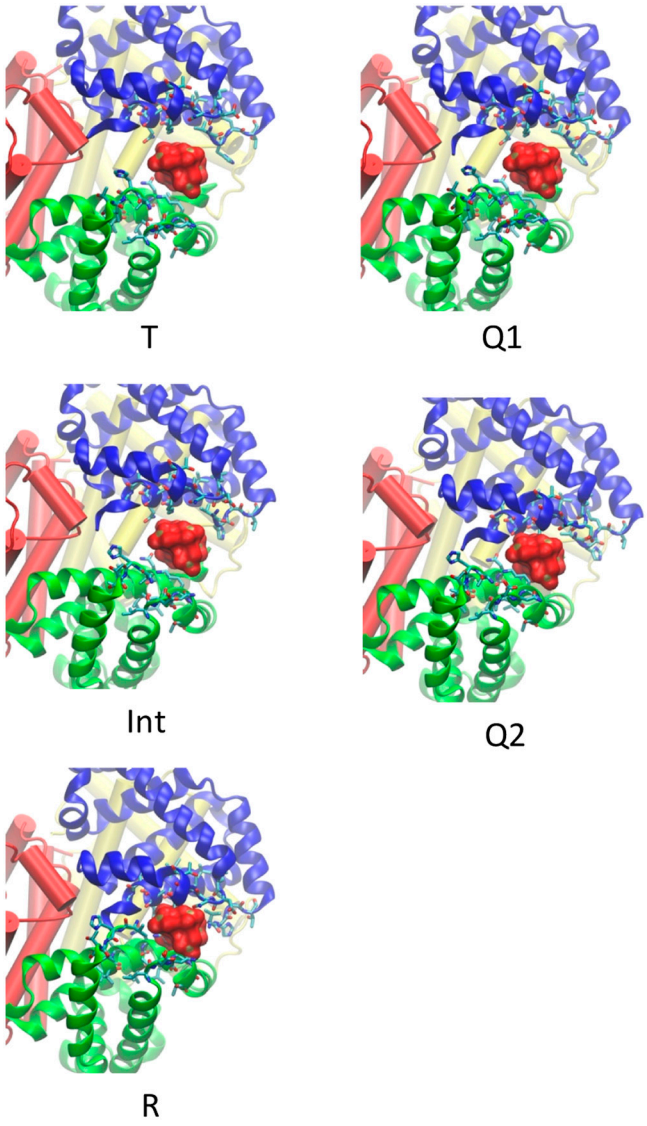

Fig. S2. Calculated interaction of hemoglobin with IHP along the CPR path. The intermediate structure ($\lambda = 0.5$) was used as a reference and the IHP molecule, shown in a surface representation, was placed in it based on orienting the IHP-bound hemoglobin X-ray structure (6) to give the best fit with the intermediate structure. The IHP was fixed and is shown where it appears in the other structures along the CPR path (T at $\lambda = 0$, Q1 at $\lambda = 0.2$, Int at $\lambda = 0.5$, Q2 at $\lambda = 0.75$, and R at $\lambda = 1$, respectively). The IHP molecule starts to overlap with hemoglobin residues after Q2, where the entrance to the central channel closes as the two β subunits rotate. These results suggest that a covalently linked IHP analog could be used to prevent Q2 and thereby trap Q1 for an X-ray structure analysis.

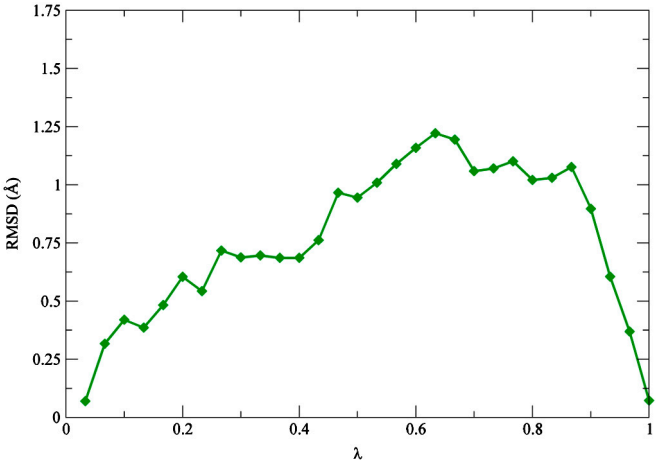

Fig. S3. Comparison with Baldwin–Chothia path. We have used the Multichain Morphed Server (1) (http://molmovdb.org/cgi-bin/beta.cgi) to determine a path for the transition that is close to the Baldwin–Chothia hypothesis. Fig. S3 shows the rmsd between structures taken from that path and from the CPR path, as a function of the transition progress (λ is defined in Fig. 2). Although the structural changes along the two paths are very different, the difference when evaluated as rmsd between structures halfway along the Baldwin–Chothia and the CPR paths is small (1.2 Å).

1. Krebs WG, Gerstein M (2000) The morph server: A standardized system for analyzing and visualizing macromolecular motions in a database framework. *Nucleic Acids Res* 28:1665–1675.

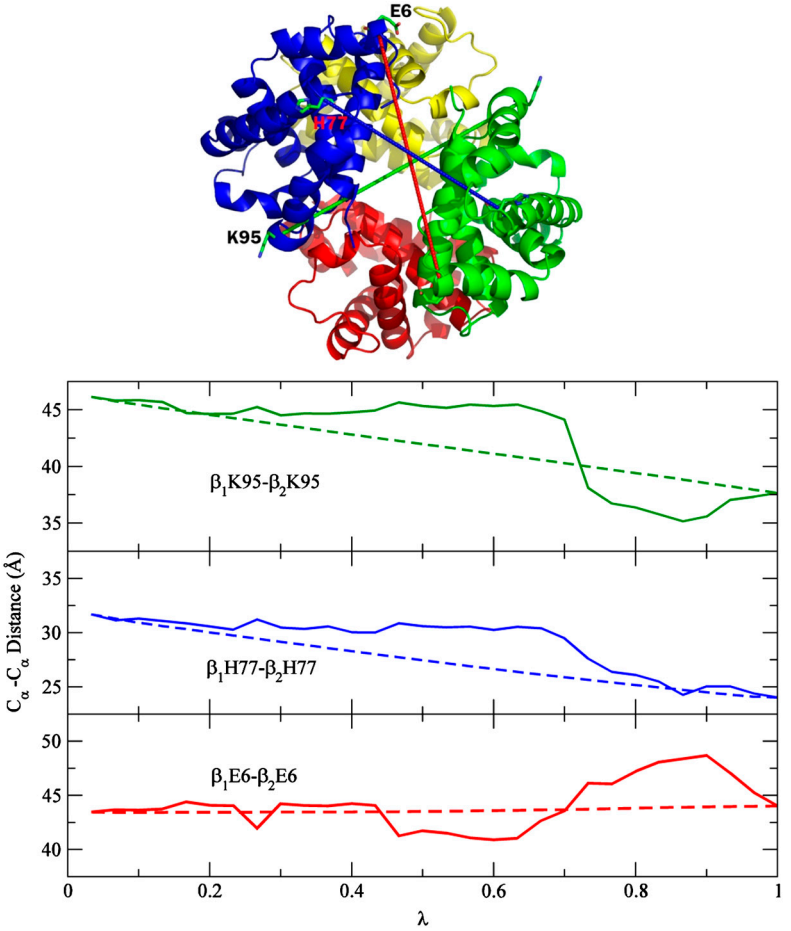

Fig. S4. Suggested FRET probes to distinguish between paths. Plotted along the transition progress (λ is defined in Fig. 2) are a number of atom–atom distances, along either the Baldwin–Chothia path (broken lines) or the CPR path (solid lines). These residues were selected so that their distances differ most between the two pathways. They are possible candidates for FRET experiments.

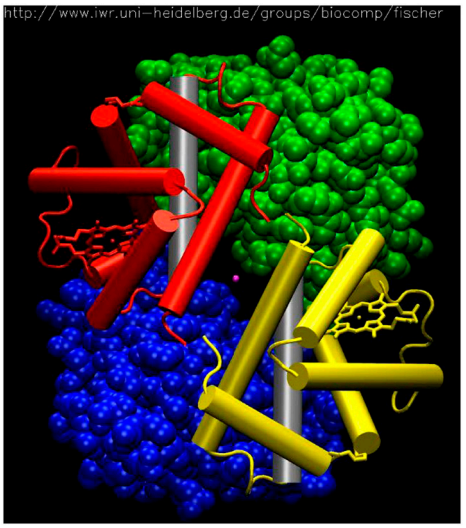

Movie S1. In the movies, the motion is shown forward and back once (the movies are better viewed with the loop mode of the movie player turned on), the subunit colors are as in the paper (α_1 in yellow, α_2 in red, β_1 in blue, β_2 in green), and the hemes are shown in licorice. Here, the view is the same as in Fig. 1*B*, down the C2 axis indicated as a purple dot (see also http://www.iwr.uni-heidelberg.de/groups/biocomp/fischer for other views). The two α-subunits counterrotate 3° around their respective αG helices (in gray), whereas the β-subunits remain stationary. Some tertiary motion (mostly of the N and C termini of the α-subunits) accompanies this quaternary event (as seen in Fig. 2*A*) and contributes to the closing of the central cavity.

Movie S1 (MOV)

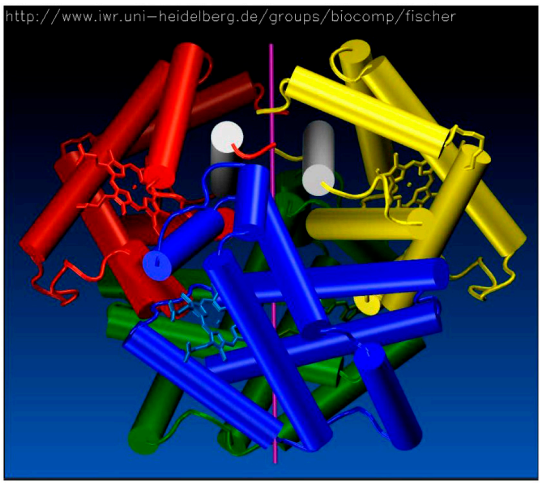

Movie S2. The view is the same as in Fig. 1*C*, orthogonal to the C2 axis (indicated as a purple line). The $\alpha_1\beta_1$- and $\alpha_2\beta_2$-dimers counterrotate 6° around their respective αH helices (in gray). Some tertiary motion (a small shift in helices αC as they glide past the βFG loop at the "switch" interface) accompanies this quaternary event (as seen in Fig. 2*A*).

Movie S2 (MOV)